# DOUBLET LATTICE METHOD FOR CALCULATIONS OF STEADY AERODYNAMIC FORCES ON GENERAL FINITE WINGS IN INCOMPRESSIBLE FLOW

Oka Sudiana
Rocket Technology Centre, National Institute of Aeronautics and Space
E-mail: oka.sudiana@yahoo.co.id

**Abstract**

Aeroelastic phenomena can occur to many engineering structures. Current design trends are aimed to engineering solutions to aeroelastic phenomena. Reliable aeroelastic analysis tools are needed to reduce expensive and time consuming experimental tests. The doublet lattice method (DLM) is one of the most powerful tools for linear flutter analyses in subsonic regime. The doublet-lattice method is still used almost exclusively for subsonic flutter clearance of flight vehicle being designed today since the high cost and technical complications with non-linear Computational Fluid Dynamics (CFD). This work are aimed to develop a computational program for calculation of steady aerodynamics force on general finite wing in incompressible regime. The present method shows good results for the steady and incompressible flow. It has been found that the results of the generalized aerodynamic forces slightly depend on the number and position composition of boxes.
**Keywords**: Aeroelastic, Aerodynamic force, Doublet Lattice Method

**Nomenclature**

| | |
|---|---|
| $\bar{w}(x,y)$ | the amplitude function of the prescribed downwash |
| $[AIC]$ | matrix of aerodynamics influence coefficient |
| $A, B$ | complex coefficients |
| $K$ | kernel function represents the contribution to downwash at field point (x,y) |
| $L$ | Length of doublet filament |
| $U$ | freestream velocity in the $x$ direction |
| $c$ | chord |
| $e$ | half of semispan |
| $p$ | pressure |
| $x,\ y,\ \xi,\ \eta$ | point of coordinate system |
| $\Lambda$ | swept angle |
| $\rho$ | density |
| $\omega$ | the circular frequency of oscillation |

## 1. INTRODUCTION

Aircraft flutter is a destructive phenomenon that requires special attention in design process [1,2,3]. Lifting-surface theory methods have been developed for the application of lifting-surface theory to wings of various configurations: planar and nonplanar wings, one wing or several, and steady and unsteady flow [4,5,6]. The singular part of the loading is not influenced by boundary conditions because of the presence of the other edges of the wing. Multhop [7]and Wagner [8] described the basis of the lifting surface theory to calculate the local lift and pitching moment at a number of chordwise sections from a set of linear equations satisfying the downwash conditions at two pivotal points in each section.

The Doublet-Lattice Method [9,10,11], has provided a robust approach for non-stationary aerodynamic prediction. An efficient state-of-the-art method called “Doublet Lattice” is described for calculating the aerodynamic loading on infinitely thin, harmonically oscillating airfoils in subsonic flow. The DLM offers a faster way of computing unsteady aerodynamic loads.

The doublet-lattice method is still used almost exclusively for subsonic flutter clearance of flight vehicle being designed today since the high cost and technical complications with non-linear Computational Fluid Dynamics (CFD) [11].

This work are aimed to develop a computational program for calculation of steady aerodynamics force on general finite wing in incompressible regime.

## 2. METHODOLOGY

The methodology of this research are divided to become several step, such as:

**Step 1: Define geometry of the wing**

The first process provides geometry and meshing of the wing. This tasks are required for analyze pressure distribution along the wing. It is the most critical for the success of the computation.
Results of this step is identify the doublet filament and control point to determine next step

**Step 2: Aerodynamic Influence Coefficients (AIC)**

The method of Aerodynamic Influence Coefficients (AIC) yields fast and reliable estimates of aerodynamic forces. After set wing model, then begins with a set of baseline modes [12,13]. From these modes an aerodynamic base is calculated.

**Step 3: Downwash**

For a lifting wing, the air pressure on the top of the wing is lower than the pressure below the wing. Near the tips of the wing, the air is free to move from the region of high pressure into the region of low pressure. The wing tip vortices produce a **downwash** of air behind the wing which is very strong near the wing tips and decreases toward the wing root. The effective angle of attack of the wing is decreased by the flow induced by the downwash, giving an additional, downstream-facing, component to the aerodynamic force acting over the entire wing [14,15].
In this step, we compute downwash that reduce lift. This downwash may effect flight stability and deformed the wing.

**Step 4: pressure distribution of deformed wing**

These loads distribution cause the bending and twisting of the wing. These deformations also change the angle of attack and consequently change the aerodynamic flow. There is an interaction between the forces and the deflections until an equilibrium condition is reached.
The interaction between the wing structural deflections and the aerodynamic loads determines the wing bending and twisting at each flight condition, and must be considered in order to model the static aeroelastic behavior [16,17].

**Step 5: generalized aerodynamic forces**

Aerodynamic forces in wing are used for analyze structure dynamics and stability. From these result, the effect of difference potential flow along upper and under thin wing can reduce lift and deformed the wing.

## 3. DOUBLET-LATTICE METHOD

The DL-method [9,10,11] is a lifting element method in which the infinitely thin lifting surfaces are divided into trapezoidal elements (panels). These elements are arranged in strips aligned with the direction of freestream. Each element contains a distribution of acceleration potential doublets, which is equivalent to a pressure jump across the surface. Each potential (pressure jump) is of oscillating yet unknown strength, concentrated at its ¼-chord line (lifting line). In addition each element possesses a control point (collocation point) in the middle of its ¾-chord line. The normal-wash introduced by all lifting lines is summed for each control point. Equalizing this to a prescribed normal-wash, as derived from the oscillatory behaviour of the lifting surface, leads to a set of algebraic equations. From these equations the strength of the lifting line and thus the pressure jump across the surface can be computed. Integration over the surface gives local and total aerodynamic force coefficients.
This calculation is restricted to planar wings [9] ($z = 0$). We have upwash equation:

$$\bar{w}(x, y, 0) = \frac{1}{4\pi\rho V} \iint_S \Delta\bar{p}\bar{K}\left((x-\xi), (y-\eta), 0\right) d\xi\, d\eta \qquad (1)$$

$$\bar{w}(x, y, 0) = \left[\frac{-\Delta p \Delta x}{4\pi\rho V}\right] \lim_{a \to 0} \int_{-s}^{s} \left[\frac{K\left((x-\xi), (y-\eta), 0\right)}{(y-\eta)^2 + a^2}\right] d\eta \qquad (2)$$

The doublet-lattice method[9] is an empirical device which simplifies the integration of the singular equation (2). The advantage gained by the doublet-lattice method is relative simplicity in the resulting computer program, especially for complex configurations. In figure 3-1,

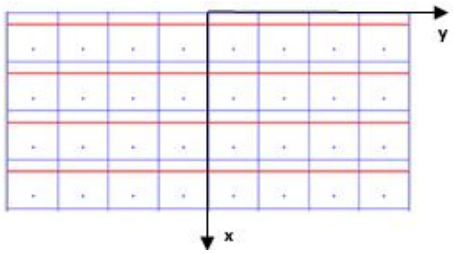


**Figure 3-1** A Rectangular Lattice

Each filament is contained in its own box. The doublet filament is placed at the ¼ chord each box. The upwash $w(x, y, 0)$ is evaluated at the ¾ chord midspan of each box. There is an empirical quality with the choice of the ¾ chord and ¼ chord. Albano and Rodden[9] take the control point at the ¾ chord measured at the box midspan, as seen in **fig. 3-2**. The flow field generated by this lattice of doublets will not be smooth, especially near the wing surface. What is important is that the upwash at the 3/4 chord is approximately the same whether one has a constant strength doublet line at the 1/4 chord.

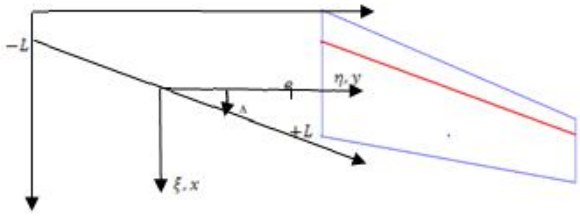


**Figure 3-2** Local a box coordinates [11]

### 3.1 Kernel function in planar wing

The Kernel function [5,6,11] can be defined as

$$\overline{K}(x_0, y_0, 0) = K_1(x_0, y_0) exp\left[\frac{-i\,\omega\, x_0}{U}\right] \quad (3)$$

Then,

$$K_1 = -I_1 - \left[\frac{M|y_0|}{(x_0^2+\beta^2 y_0^2)^{\frac{1}{2}}}\right]\left[\frac{\exp(-ik_1 u_1)}{(1+u_1^2)^{\frac{1}{2}}}\right] \quad (4)$$

$$I_1 = \int_{u_1}^{\infty}\left[\frac{\exp(-ik_1 u_1)}{(1+u_1^2)^{\frac{3}{2}}}\right] du \quad (5)$$

where

$$k_1 = \frac{\omega r_1}{U} \quad (6)$$

$$u_1 - \frac{-x_0+M\bar{R}}{r_1\beta^2} \quad (7)$$

$I_1$ can be abbreviated as:

$$I_1 = \exp(-ik_1 u_1)\left[1 - \left(\frac{u_1}{(1+u_1^2)^{\frac{1}{2}}}\right) + (-ik_1 J_1)\right] \quad (8)$$

Where

$$J_1 = \exp(-ik_1 u_1)\int_{u_1}^{\infty}\left[1 - \left(\frac{u_1}{(1+u_1^2)^{\frac{1}{2}}}\right)\right]\exp(-ik_1 u_1)\, du \quad (9)$$

Lascha [18] provides the formula accurate approximation for $u_1 \geq 0$, which is

$$\left[1 - \left(\frac{u_1}{(1+u_1^2)^{\frac{1}{2}}}\right)\right] \approx \sum_{n=1}^{11} a_n e^{-nc u_1} \quad (10)$$

Substitute equation (10) into equation (9) to obtain an approximation of $J_1$

$$J_1 \approx \sum_{n=1}^{11}\left[\frac{a_n e^{-nc u_1}}{n^2c^2 + k_1^2}\right](nc - ik_1) \quad (11)$$

This formula is valid only for $u_1 \geq 0$. Taking advantage of symmetry of integrand, for $u_1 < 0$ can be defined as:

$$I_1(u_1,k_1) = 2Re[I_1(0,k_1)] - Re[I_1(-u_1,k_1)] + iIm[I_1(u_1,k_1)] \quad (12)$$

Where

$$I_1(0,k_1) = 1 + (-ik_1 J_{10}) \quad (13)$$

$$J_{10}(0,k_1) \approx \sum_{n=1}^{11} \left[\frac{a_n}{w^2c^2 + k_1^2}\right](nc - ik_1) \quad (14)$$

$\overline{K}$ is a complex function. It turns out that $\overline{K}$ can be approximated with a complex parabolic function of $\eta$.

$$\overline{K}(x_0,y_0) = A_0 + A_1\eta + A_2\eta^2 \quad (15)$$

Where $A_0, A_1$, and $A_2$ are complex coefficients.

- The coordinate $(x_L, y_L)$ stands for $(x_0, y_0)$ at $\eta = -\varepsilon$.
- The coordinate $(x_R, y_R)$ stands for $(x_0, y_0)$ at $\eta = \varepsilon$
- The coordinate $(x_C, y_C)$ stands for $(x_0, y_0)$ at $\eta = 0$.

Equation (15) can be defined as

$$\overline{K}(x_0,y_0) = \left[\frac{\eta(\eta-\varepsilon)}{2\varepsilon^2}\right]\overline{K}(x_L,y_L) + \left[\frac{\varepsilon^2-\eta^2}{\varepsilon^2}\right]\overline{K}(x_C,y_C) + \left[\frac{\eta(\eta+\varepsilon)}{2\varepsilon^2}\right]\overline{K}(x_R,y_R) \quad (16)$$

Thus, it can be identified that the coefficients in equation (16) as

$$\left.\begin{aligned} A_0 &= \overline{K}(x_C,y_C) \\ A_1 &= \frac{\overline{K}(x_R,y_R) - \overline{K}(x_L,y_L)}{2\varepsilon} \\ A_2 &= \frac{\overline{K}(x_R,y_R) + \overline{K}(x_L,y_L) - 2\overline{K}(x_C,y_C)}{2\varepsilon^2} \end{aligned}\right\} \quad (17)$$

To determine $A_0$, $A_1$, $and$ $A_2$, it is necessary to compute

$$\left.\begin{aligned} \overline{K}(x_R,y_R,0) &= K_1(x_R,y_R)exp\left[\frac{-i\omega x_R}{U}\right] \\ K(x_C,y_C,0) &- K_1(x_C,y_C)exp\left[\frac{-i\omega x_C}{U}\right] \\ K(x_L,y_L,0) &- K_1(x_L,y_L)exp\left[\frac{-i\omega x_L}{U}\right] \end{aligned}\right\} \quad (18)$$

By substituted $\overline{K}$ in equation (16) into equation (2), and performing the integration, it is obtained

$$\overline{w}(x,y,0) = \left[\frac{-\Delta p\Delta x}{4\pi\rho U}\right]\lim_{\varepsilon \to 0}\int_{-\varepsilon}^{\varepsilon}\left[\frac{A_0 + A_1\eta - A_2\eta^2}{(y-\eta)^2 + \epsilon^2}\right]d\eta$$

$$\overline{w}(x,y,0) - \frac{-\Delta p\Delta x}{4\pi\rho U}[D_0 + D_1 + D_2] \quad (19)$$

For validation of the code is needed to consider the case of different values of Mach number ($M$) and reduced frequency ($k$). In this case, some result is given for the steady case ($k$=0) and the incompressible case ($M$=0). From the eq. (4) and (8), for case for the steady and the incompressible case, can be abbreviated as:

$$K_1 = -I_1 \quad (20)$$

Then,

$$I_1 = 1 - \left(\frac{u_1}{(1+u_1^2)^{\frac{1}{2}}}\right) \quad (21)$$

And,

$$u_1 - -\frac{x_0}{|y_0|} \quad (22)$$

### 3.2 Aerodynamic Influence Coefficients (AICs)

Typical linear aeroelastic analysis using DLM evaluates complex-valued Aerodynamic Influence Coefficients (AICs). The method of Aerodynamic Influence Coefficients (AIC) yields fast and reliable estimates of aerodynamic forces and, because of this, is widely used in aeroelastic analysis applications. The AIC method begins with a set of baseline modes being obtained for the wing model. From these modes an aerodynamic base is calculated.

The AIC method begins with a set of baseline modes being obtained for the wing model. From equation (19), the equation can be followed

$$\bar{w}(x,y,0) = \frac{-\Delta y \Delta x}{4\pi\rho U}[AIC] \qquad (23)$$

Which

$$[AIC] = [B_0 + B_1 + B_2] \qquad (24)$$

The definitions of $B_0, B_1,$ and $B_2$ are given as

$$B_0 = \left[\frac{2eA_0}{y^2 - e^2}\right]$$

$$B_1 = A_1\left[\frac{1}{2}log\left[\frac{(e-y)^2}{(e+y)^2}\right] + \left[\frac{2ey}{y^2 - e^2}\right]\right] \qquad (25)$$

$$B_2 = A_2\left[2e + (y)log\left[\frac{(e-y)^2}{(e+y)^2}\right] + \left[\frac{2ey^2}{y^2 - e^2}\right]\right]$$

When a flutter analysis has been completed, one must assure that the box resolution is adequate to capture the frequency of instability. The required box density depends on a combination of wing deformation and the frequency of motion. It should be increased as the deformation becomes more spatially wavy and as the temporal frequency of motion increases.

## 4. RESULTS AND DISCUSSIONS

### 4.1 The Steady and incompressible flow

The test cases for the computations with present method are at swept wing with $\Lambda_{LE} = 45\ deg$ , $AR - 1.5, \lambda - 1/7, \bar{w}/U - -1.0$. This calculation is done with some variation of the number of boxes. From **table 4-1**, we can see with change the number of boxes in rows along x-axis and no change the number of boxes in columns along y-axis, lift coefficient increase. Contrary if the number of boxes in rows are less than in columns. Needs good combination of the number of boxes in rows and column to obtain good result

**Table 4-1.** Computational result using present method for several sequence number of the boxes.

| Number Boxes | Lift Coeff., Cl; |
|---|---|
| 2 x 5 | 3.2405 |
| 4 x 5 | 3.3391 |
| 8 x 5 | 3.4314 |
| 8x10 | 3.2196 |
| 10x12 | 3.2001 |

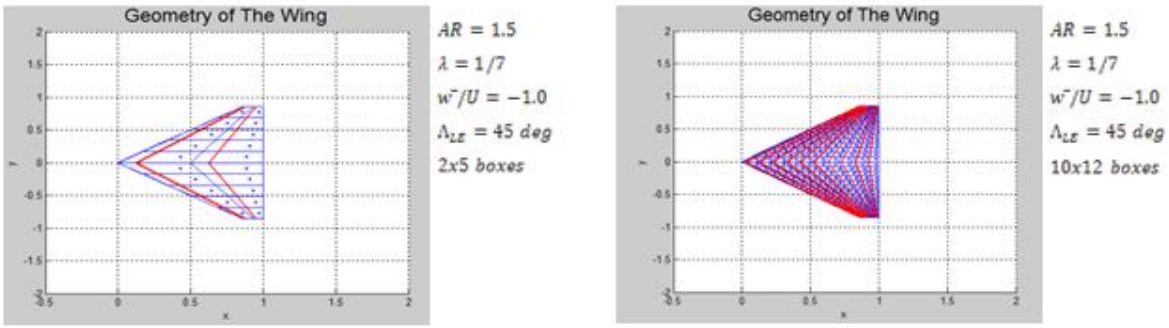


**Figure 4-1**. The swept wing with various number of the panel/boxes ($\Lambda_{LE} = 45\,deg$, $AR = 1.5$, $\lambda = 1/7$)

The geometries of the wing with mesh or the number of boxes can be seen in **Figure. 4-1**. This geometries show the wing mesh with a 45-deg leading-edge swept, an aspect ratio $A$R=1.5, a tape ratio $\lambda$=1/7, reduced frequency $k$=0, and downwash, $w/U$=−1.0 with variation of the number of boxes. Increasing the number of boxes is to obtain precisely result.

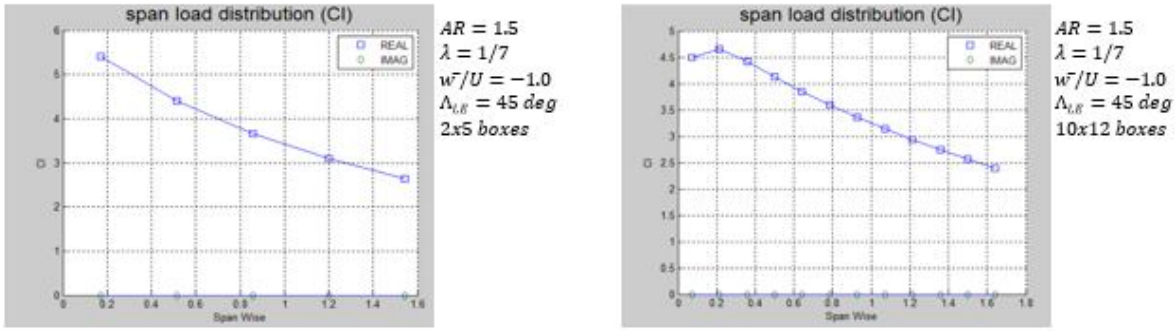


**Figure 4-2.** The span load distribution for the swept wing, various number of the panel/boxes ($\Lambda_{LE} = 45\,deg$, $AR = 1.5$, $\lambda = 1/7$, $k = 0$, $M = 0$, $w/U = -1.0$)

From **figure 4-2** shows the comparison the span load distribution for a swept wing with a 45-deg leading-edge swept, an aspect ratio of 2, a taper ratio $\lambda$=1/7, reduced frequency $k$=0, and downwash , $w/U$=−1.0 for various the number of boxes for the steady and incompressible flow. The graphs decrease when the number of panel/boxes are increased. The trend of graph are slightly equal.

The comparison of the pressure distribution for a swept wing for various the number of boxes for the steady and incompressible flow can be seen in **figure 4-3**. The graphs decrease when the number of panel/boxes are increased.

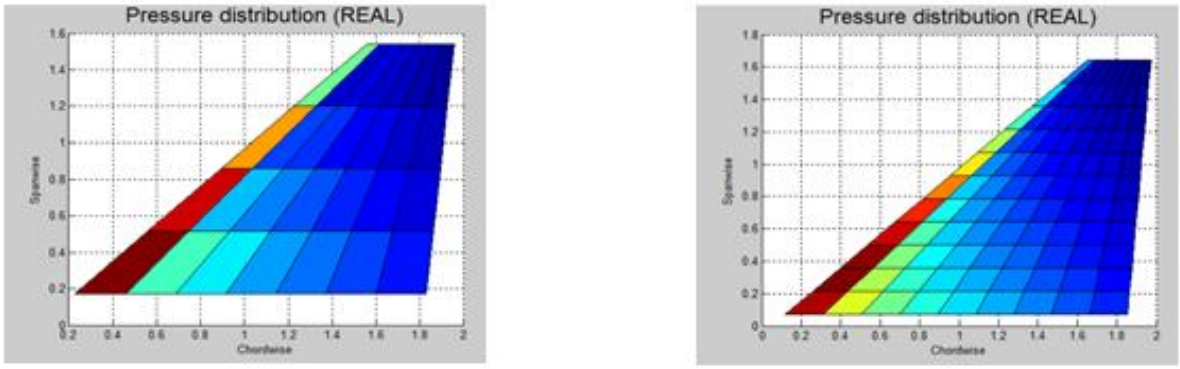


**Figure 4-3**. The comparison of the pressure distribution for the swept wing, real value, various number of the panels/boxes ($\Lambda_{LE} = 45\,deg$, $AR = 1.5$, $\lambda = 1/7$, $k = 0$, $M = 0$, $w/U = -1.0$)

We need to validate the present result, we compare this result with literature in reference [19]. Hedman [19] consider the wing surfaces divided in the chordwise and spanwise directions into panel or boxes. Hedman [19] simulate the panel load with a horseshoe vortex, and the boundary condition is fulfilled on every panel at one point. For each surface, the vertice and the control points are located on a wing chord plane.

**Table 4-1** The comparison of lift coefficient between the present method and Hedman [19] (the steady and incompressible flow)

| Number Boxes | Lift Coeff., Cl; present | Lift Coeff., Cl; [Ref. 19] | percentage |
|---|---|---|---|
| 2 x 5 | 3.2405 | 3.2 | 1.27 |
| 4 x 5 | 3.3391 | 3.2 | 4.35 |
| 8 x 5 | 3.4314 | 3.2 | 7.23 |
| 8x10 | 3.2196 | | 0.61 |
| 10x12 | 3.2001 | | 0 |

Table 4-1 shows comparison of coefficient lift between present method and Hedman [19] with various number of boxes or panel. From this Table, The Result are obtained from present method are increase when number of boxes are raise, contrary with result from Hedman [19] which are constant when the number of boxes in chordwise are raise. Thus, the result in the present method is equal with result from Hedman[19], with more boxes. It is mean that to obtain slightly equal result, present method need more boxes than Hedman[19] because present method use lower order computation than Hedman [19].

## 5. CONCLUSION

The present method shows good results and accuracy with deviation less than 7.5 percentage for the steady and incompressible flow. It has been found that the results of the generalized forces slightly depend on the number of boxes. The present method needs more boxes to obtain equal results. This is because the doublet lattice is a lower order method compared to the vortex lattice.

## ACKNOWLEDGEMENTS

I would like to thank Professor Pablo Garcia Fogeda Nuñez from Universidad Politecnica de Madrid, whose enlightening guide me into my work. Warm thank to Moh. Risdaya Fadil from Voith 3 Aerospace, for explain more about aeroelastic field in Aerospace Industry and support me to explore structure dynamics problems. Grateful thank to Singgih Satrio Nugroho from Bandung National of Polytechnic, for help to develop the matlab code for the better.

## REFERENCES

1) Garrick, I. E., and Wilmer H. Reed III. "Historical development of aircraft flutter." *Journal of Aircraft* 18, no. 11 (1981): 897-912.
2) Kehoe, Michael W. "A historical overview of flight flutter testing." (1995).
3) Lee, B. H. K., and A. Tron. "Effects of structural nonlinearities on flutter characteristics of the CF-18 aircraft." *Journal of Aircraft* 26, no. 8 (1989): 781-786.
4) Giesing, Joseph P. *Lifting surface theory for wing-fuselage combinations*. No. DAC-67212-Vol-1. DOUGLAS AIRCRAFT CO LONG BEACH CALIF, 1968.
5) Landahl, M. T. "Kernel function for nonplanar oscillating surfaces in a subsonic flow." *AIAA Journal* 5, no. 5 (1967): 1045-1046.
6) Landahl, Marten T., and Valter JE Stark. "Numerical lifting-surface theory-Problems and progress." *AIAA Journal* 6, no. 11 (1968): 2049-2060.
7) Multhopp, H. *Methods for calculating the lift distribution of wings: Subsonic lifting surface theory*. Ministry of Supply, Royal Aircraft Establishment, RAE Farnborough, 1950.
8) Wagner, Siegfried. "On the singularity method of subsonic lifting-surface theory." *Journal of Aircraft* 6, no. 6 (1969): 549-558.

9) Albano, Edward, and William P. Rodden. "A doublet-lattice method for calculating lift distributions on oscillating surfaces in subsonic flows." *AIAA journal* 7, no. 2 (1969): 279-285.
10) Kalman, T. P., William P. Rodden, and J. P. Giesing. *Application of the doublet-lattice method to nonplanar configurations in subsonic flow,* Journal of Aircraft 8, no. 6 (1971): 406-413.
11) Blair, Max. *A compilation of the mathematics leading to the doublet lattice method*. No. WL-TR-92-3028. WRIGHT LAB WRIGHT-PATTERSON AFB OH, 1992.
12) Brink-Spalink, J., and J. M. Bruns. *Correction of unsteady aerodynamic influence coefficients using experimental or CFD data*, In International Forum on Aeroelasticity and Structural Dynamics, pp. 175-182. 2001.
13) Rodden, William P. *Aerodynamic Influence Coefficients From Strip Theory*, 2012.
14) Watkins, Charles E., Harry L. Runyan, and Donald S. Woolston. *On the kernel function of the integral equation relating the lift and downwash distributions of oscillating finite wings in subsonic flow,*1955.
15) Abbott, Ira Herbert. *Theory of wing sections, including a summary of airfoil data*. Courier Corporation, 1959.
16) Labrujere, Th E., W. Loeve, and J. W. Slooff. *An approximate method for the calculation of the pressure distribution on wing-body combinations at subcritical speeds*. Nationaal Lucht-en Ruimtevaartlaboratorium, 1970.
17) Woodward, F. A. *An improved method for the aerodynamic analysis of wing-body-tail configurations in subsonic and supersonic flow. Part 2: Computer program description*, 1973.
18) Laschka, B., *Zur Theorie der harmonic schwingen den tragen den FlächebeiUnterschallanströmung*, ZeitschriftfürFlugwissenschaften, Vol. II, No. 7, 1963, pp 265-292
19) Hedman, Sven G. *Vortex lattice method for calculation of quasi steady state loadings on thin elastic wings in subsonic flow*. No. FFA-105. Aeronautical Research Inst Of Sweden Stockholm, 1966.